# Drying-induced roughness formation on liquid film surfaces: a lubrication model of surface-tension-drive flow

M. Yamamura, T. Uchinomiya, Y. Mawatari and H. Kage
Department of Applied Chemistry, Kyushu Institute of Technology
Tobata, Kitakyushu, Fukuoka 804-8550 JAPAN

## Abstract

An air impingement onto a thin liquid layer often promotes uneven surface topographies, especially in thick, dilute polymeric coatings. Here we performed numerical simulations of drying-induced roughness formation assuming a steady but non-uniform surface temperature profile determined by the local heat balance in the liquid film. At the impinging point, the coating surface exhibits a lower temperature, and thus a higher surface tension because of the latent heat loss due to the faster solvent evaporation. The resulting surface-tension gradient drives flows to form a particular surface roughness, depending on the impinging air velocity, coating viscosity, air humidity and substrate speed.

## 1. Introduction

A large number of optical coating applications require a planar, smooth, and defect-free liquid layer. However, thin liquid films are subject to surface tension gradients in the presence of non-uniform interfacial temperature and/or concentration. The surface tension gradients promote interfacial Marangoni stresses that tend to move the fluid from low surface tension regions to high surface tension regions, leading to a noticeable deformation of the film surface. In contrast, the capillary and sometimes gravitational forces tend to reduce irregularities in the coating layer. Opposing these forces is viscous stress that can increase as a solvent evaporates. The subtle balance of these forces generally promotes characteristic topographical changes, depending on the operating conditions in a complicated manner. Extensive studies have focused on thin film flows based on the lubrication theory. For isothermal coatings, Joos (1996) investigates the levelling of multiple stratified layers of different viscosities. Weidner et al. (1999) developed a mathematical model for the liquid layer coated on a curved surface, and Eres et al. (1999) performed three-dimensional numerical simulations of the levelling of liquid layers assuming that the evaporation rate varies as a power of the liquid composition. Considering a constant evaporation rate until the mixture is dry, Evans et al. (2000) solved the film evolution equation coupled with the local concentration profile across the coating to predict crater defect formation. For non-isothermal coatings, Gramlich et al. (2002) numerically investigated the optimal levelling of the ridge by a thermo-capillary stress. Blunk and Wilkes (2001) and recently Edmonstone and Matar (2004) considered the simultaneous effects of thermal and surfactant-driven Marangoni stresses on the thin film evolution. The effects of thermo-capillarity, evaporation and Van der Waals forces on the long-scale film evolution are summarized by Oron et al. (1997).
However, characteristics of the surface deformation in industrial airflow driers are still poorly understood. In general, turbulent airflows were impinged onto an evaporating coating from the series of slit air nozzles. The air impingement promotes a local variation in evaporation rate, and thus the temperature/concentration distributions along the drying surface. The major interesting feature is that the resulting surface tension gradient periodically varies as the coating passes beneath the impinging air flows. If the travelling time between the nozzles is much shorter than the time required for the surface deformation, the roughness can completely level before the coating passes under the following nozzle. At higher coating speed, on the contrary, the coating does not level during a finite drying time. In this paper we applied the film evolution theory to the drying-induced surface roughness formation in the airflow driers. For simplicity, the surface tension is assumed to vary with surface temperature as has been done in the literature. The numerical simulations showed a characteristic axisymmetric coating thickness profile on a stationary substrate, whereas it becomes asymmetric and periodically grew and decayed with time on a moving substrate.

## 2. Lubrication model

Consider a thin liquid film of incompressible Newtonian fluid of viscosity $\mu$ coated with a uniform thickness of $h$ on a horizontal substrate. The deformable air-liquid interface locates at $z=h(x, t)$ where $z$ and $x$ are the Cartesian coordinates in the thickness and transverse directions, respectively. The velocity distribution

within the film is defined as $u(x, z)$ with origin on the film–substrate interface directly beneath the air impinging point. Using a linear approximation for the surface tension with respect to temperature, we obtain $\sigma=\sigma_0-\gamma(T-T_0)$, where $T_0$ and $\sigma_0$ denote the reference temperature and surface tension. The surface tension gradient, $\gamma$, is positive and assumed to be constant in the temperature range of interest. For simplicity, the surface tension gradient with respect to the solvent concentration is assumed to be negligible. The stress boundary condition for the velocity at the free surface is given by:

$$\mu\frac{\partial u}{\partial z}=\frac{d\sigma}{dx} \qquad (1).$$

No slip boundary condition at $z=0$ gives $u=0$. Using the lubrication approximation and neglecting inertia and gravity, the equations of motion in x and z directions yield:

$$\frac{\partial p}{\partial x}=\mu\frac{\partial^2 u}{\partial z^2} \qquad (2), \qquad \frac{\partial p}{\partial z}=0 \qquad (3)$$

Thus the local liquid pressure $p$ is independent of $z$. The lubrication approximation is valid for small topographic changes of the surface profile. Assuming the sufficiently small slope of the free surface, an approximate form for the free surface curvature yields,

$$p=-\sigma\frac{\partial^2 h}{\partial x^2} \qquad (4)$$

Integrating the parabolic velocity profile in the $z$-direction gives the total flux $Q$ at a given position $x$.
The mass conservation law gives:

$$\frac{\partial h}{\partial t}=-\frac{\partial Q}{\partial x} \qquad (5)$$

Combining these equations yields a non-linear evolution equation for the film thickness $h$ as:

$$\frac{\partial h}{\partial t}=-\frac{\partial}{\partial x}\left[\frac{h^3}{3\mu}\frac{\partial}{\partial x}\left(\sigma\frac{\partial^2 h}{\partial x^2}\right)+\frac{h^2}{2\mu}\frac{\partial\sigma}{\partial x}\right] \qquad (6)$$

The viscosity is taken to depend exponentially on the bulk polymer concentration $C$ [wt%]. For simplicity, we assumed that the time scale for diffusion is much shorter than that for drying, and hence, the polymer concentration is assumed to be uniform across the coating. The viscosity measurements for poly-vinyl-alcohol/water solutions give:

$$\mu=\begin{cases}0.0004899\,e^{0.7782\,C} & at \quad C(wt\%)<6\\ 0.05223\,e^{0.4486\,(C-6)} & at \quad C(wt\%)\geq 6\end{cases} \qquad (7)$$

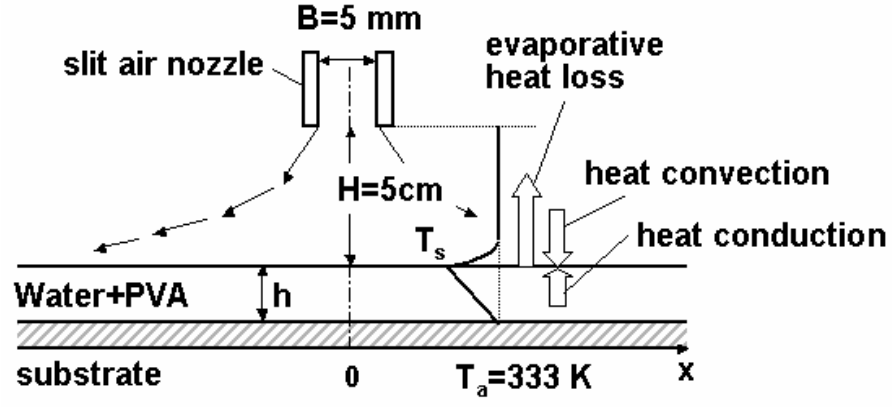


Figure 1 Initial configuration of the evaporating coating on the plane substrate.

Neglecting the heat conduction in the $x$ direction, the steady temperature profile along the surface was obtained from the local energy balance (Figure 1):

$$\frac{k^G M}{RT_s}\Delta H(P_s-P_a)=h^G(T_a-T_s)+\frac{\lambda}{h}(T_a-T_s) \qquad (8)$$

where $h$ is the film thickness, $M$ the solvent molecular weight, $P_a$ the saturated solvent pressure in gas phase, $T_s$ the surface temperature, and $\lambda$ the liquid heat conductivity. The first and the second terms on the right hand side represent the heat convection from the surrounding air, and heat conduction from the substrate to the coating, respectively, whereas the left hand side denotes the evaporative heat loss. The saturated vapour pressure at the surface $P_s$ is assumed to be constant for the sake of simplicity. $h_G$ and $k_G$ in Eq. (8) are the

heat and mass transfer coefficients obtained from the empirical correlations based on the boundary layer theory for the impinging slit flow as:

$$Nu_x(=\frac{h^G B}{\lambda^G}) = 0.06958\,\mathrm{Re}^{0.8}\,\mathrm{Pr}^{0.43}(\frac{x}{H})^{-0.37}(\frac{H}{B})^{-0.62} \qquad (9)$$

$$Sh_x(=\frac{k^G B}{D}) = 0.06958\,\mathrm{Re}^{0.8}\,Sc^{0.43}(\frac{x}{H})^{-0.37}(\frac{H}{B})^{-0.62} \qquad (10)$$

$$Nu_0(=\frac{h^G B}{\lambda^G}) = 1.42\,\mathrm{Re}^{0.58}\,\mathrm{Pr}^{0.43}(\frac{H}{B})^{-0.62} \qquad (11)$$

$$Sh_0(=\frac{k^G B}{D}) = 1.42\,\mathrm{Re}^{0.58}\,Sc^{0.43}(\frac{H}{B})^{-0.62} \qquad (12)$$

where the Reynolds number is defined with respect to the outflow air velocity and the slit width. The cut-off values from Eqs. (11)–(12) were applied beneath the air nozzle because the transfer coefficients calculated from Eqs. (9) –(10) give infinite values at the impinging point *x=0*.

Combining Eqs. (8) –(12) yields the steady temperature profile along the evaporating surface. Substituting the temperature and thus the resulting surface tension variations into Eq. (6) gives the time-evolution of the coating thickness profile. For coating on a moving substrate, the temperature profile was numerically moved at a constant speed in order to simulate the coating motion. Eq. (6) was discretized and solved numerically using the finite difference method. The time integration was done using fully explicit scheme with sufficiently small time steps to ensure the numerical stability. The parameters chosen are thought to be representative of real drying conditions as $B$=5 mm, $H$=5 cm, $T_a$=333 K, $\lambda^G$= 0.0276 J/(m·sK), $\lambda$ = 0.657 J/(m·sK), D=3.2×10$^{-5}$ m$^2$/s, $M$=18 g/mol, and $\Delta H$=2260 kJ/kg.

## 3. Results and discussions

### 3.1 Film evolution on a stationary substrate

First we demonstrated the evolution of thin liquid films coated on a stationary substrate. Figure 2a shows the variation in surface tension obtained from the computed steady temperature profile along the coating surface. The surface tension exhibits a peak near the air impinging point (*x=0*) and decreases as the thermal boundary layer develops along the free surface. The flat surface tension profile beneath the nozzle corresponds to the cut-off heat/mass transfer coefficients in Eqs. (11) – (12). The surface tension gradient induces the interfacial stress to promote a particular surface roughness. As found from Figure 2b, the initially uniform coating begins to show a crest and two troughs with a particular increasing pitch.

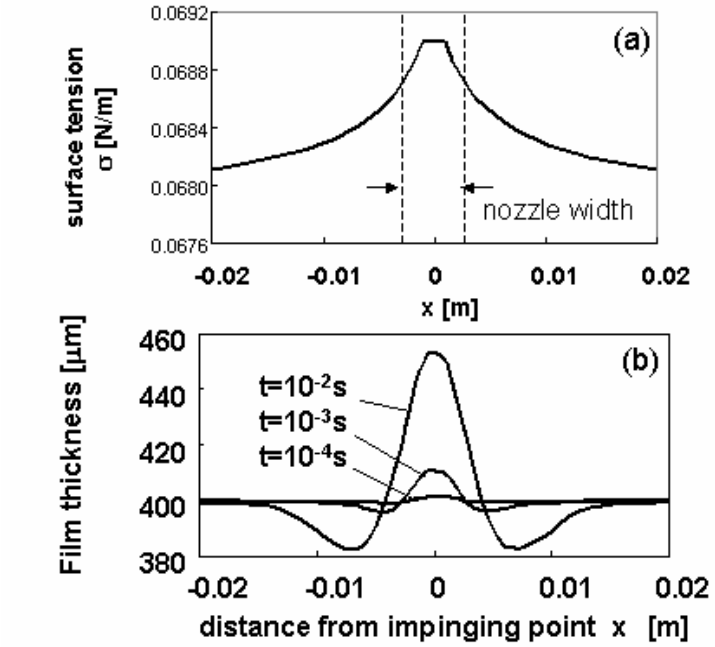


Figure 2 The surface tension and film thickness profiles of liquid films coated on a stationary substrate.

The characteristic surface roughness formation is attributed to the interfacial Marangoni stress that competes against the levelling flow. The crest grows as the stress drags the fluid from the surrounding low surface tension region to the high surface tension region at the impinging point. The mass continuity leads to formation of deep troughs that also grow as the coating dries. On a stationary substrate, the crest and troughs grow until the competing capillary and viscous forces become comparable to the Marangoni stress.

### 3.2 Film evolution on a moving substrate

We next demonstrated how the liquid film evolves on a moving substrate. Figure 3 shows a comparison of the film profiles between coatings on a stationary and a moving substrate. For the latter, the coating moves from the left to the right with a constant speed of 0.5 m/s. In contrast to the axisymmetric thickness distribution on a stationary substrate, the coating on a moving substrate exhibits a particular asymmetric profile. Furthermore, the crest height at the peak was significantly reduced as the substrate speed increases.
Figure 4 shows the time-variations in surface temperature and thickness of the liquid film coated on a moving substrate. The asymmetric surface profile moves as the coating passes beneath the air nozzle. The film thickness increases and decreases with time at a fixed position on the *x* coordinate, showing a periodic growth and decay of the surface topography in the airflow drier.

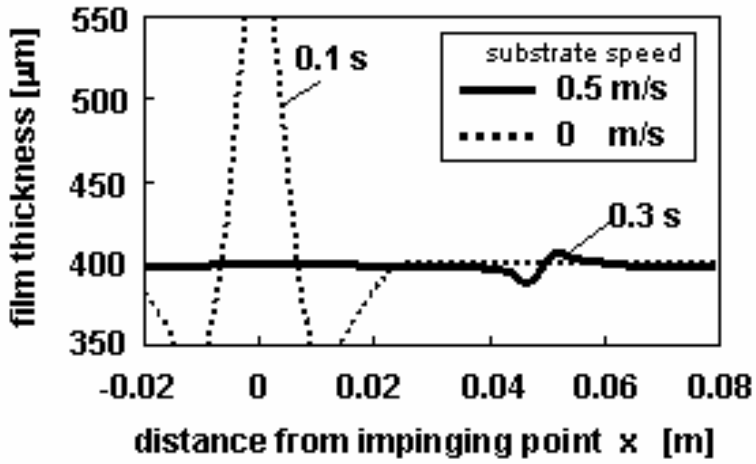


Figure 3 Comparison of the surface profiles between coatings on a stationary and a moving substrates. The initial film thickness is 400 μm, air inlet velocity is 10 m/s, air temperature is 333 K, relative humidity is 0 %, initial PVA weight fraction is 2 wt%.

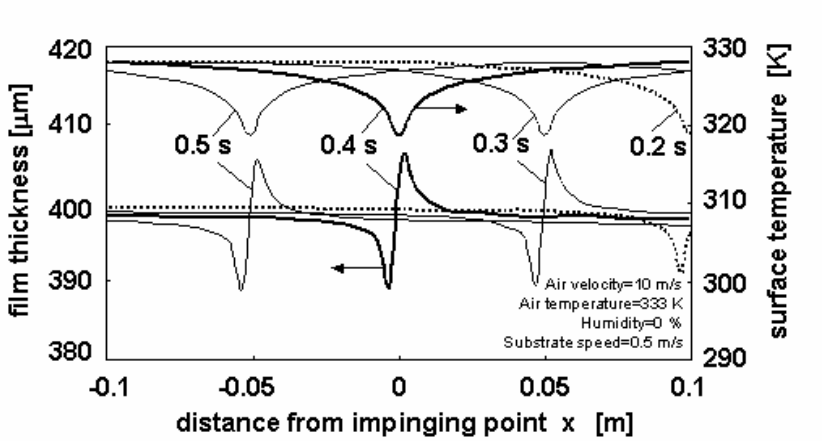


Figure 4 The time evolution of the surface profiles on a moving substrates. The initial film thickness is 400 μm, air inlet velocity is 10 m/s, air temperature is 333 K, relative humidity is 0 %, initial PVA weight fraction is 2 wt%, and the substrate speed is 0.5 m/s.

To characterize the surface roughness in a quantitative sense, we computed the maximum surface roughness $(h_{max}-h_{min})/h_0$ and the trough pitch, $x_{max}-x_{min}$, where $h_{max}$, $h_{min}$, and $h_0$ represent the maximum film thickness at the crest, minimum thickness at the trough and the initial film thickness, respectively. $x_{max}$ and $x_{min}$ are the $x$ positions at which the coating involves the troughs. Figure 5 shows the variation in maximum surface roughness on the air velocity. The surface roughness exhibits two distinct regimes. The roughness increases with increasing impinging air velocity at low air velocities (regime I), whereas higher air velocities retard the roughness formation at relatively high velocity regimes (regime II). The former is attributed to the Marangoni effect, while the latter possibly stems from the strong capillary pressure, and thus the strong levelling flow, at the cooler crest. Figure 6 shows the effect of air velocity on the trough pitch. Increasing air velocity directly leads to the monotonic increase in pitch. These results suggest that, above the critical air velocity between regime I and regime II, higher air velocities can give rise to a smoother coating surface with a longer trough pitch, showing some directions for reducing the surface roughness within shorter drying times.

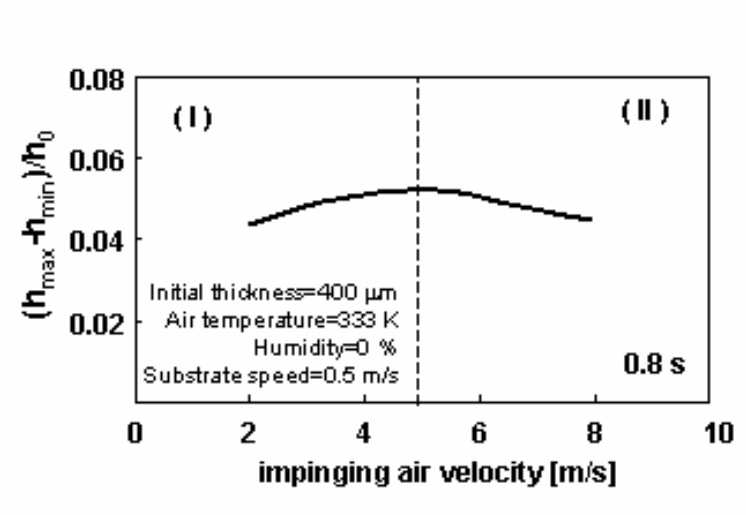


Figure 5 The effect of impinging air velocity on the maximum surface roughness. The roughness first increases (regime I) and then decreases (regime II) with increasing air velocity. The initial film thickness is 400 μm, air temperature is 333 K, relative humidity is 0 %, initial PVA weight fraction is 2 wt%, substrate speed is 0.5 m/s and the elapsed drying time is 0.8 s.

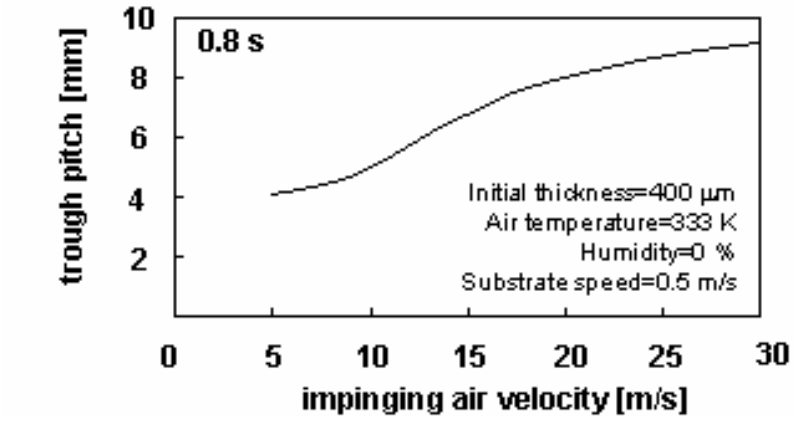


Figure 6 The effect of impinging air velocity on the trough pitch. The pitch monotonically increases as the air velocity increases. The initial film thickness is 400 μm, air temperature is 333 K, relative humidity is 0 %, initial PVA weight fraction is 2 wt%, substrate speed is 0.5 m/s and the elapsed drying time is 0.8 s.

## 4. Conclusions

We carried out numerical simulations for the uni-directional lubrication flow in the air-impinging driers. The evaporative cooling results in a cooler surface temperature beneath the air impingement, leading to a surface-tension gradient that induces Marangoni stresses. The interfacial stress promotes an axisymmetric thickness

profile for the liquid films coated on a stationary substrate. The initially uniform coating begins to show a particular crest and two troughs. On a moving substrate, on the contrary, the thickness profile becomes asymmetric depending on the substrate speed. The asymmetric surface topography periodically grows and decays as the coating passes beneath the impinging airflow. Numerical results revealed that, above the critical air velocity, higher air velocities give rise to a smoother coating surface with a longer trough pitch.

## 5. References


1. Joos, F. M. Leveling of a film with stratified viscosity and insoluble surfactant, *AIChE Journal*, **42**, 623-637 (1996)
2. Weidner, D. E.; Schwartz, L. W. and Eley, R. R. Role of surface tension gradients in correcting coating defects in corners, *Journal of Colloid and Interface Science*, **179**, 66-75 (1996)
3. Eres, M. H.; Weidner, D. E. and Schwartz, L. W. Three-dimensional direct numerical simulation of surface-tension-gradient effects on the levelling of an evaporating multicomponent fluid, *Langmuir*, **15**, 1859-1871 (1999)
4. Evans, P. L.; Schwartz, L. W. and Roy, R. V. A mathematical model for crater defect formation in a drying paint layer, *Journal of Colloid and Interface Science*, **227**, 191-205 (2000)
5. Gramlich, C. M.; Kalliadasis, S. ; Homsy, G. M. and Messer, C. Optimal levelling of flow over one-dimensional topography by Marangoni stresses, *Physics of Fluids*, **14**, 1841-1850 (2002)
6. Blunk, R. H. J. and Wilkes, J. O. Computational analysis of surface-tension-driven coating-defect flow, *AIChE Journal*, **47**, 779-789 (2001)
7. Edmonstone, B. D. and Matar, O. K. Simultaneous thermal and surfactant-induced Marangoni effects in thin liquid films, *Journal of Colloid and Interface Science*, **274**, 183-199 (2004)
8. Oron, A.; Davis, S. H. and Bankoff, S. G. Long-scale evolution of thin liquid films, *Reviews of Modern Physics*, **69**, 931-980 (1997)